Classification
Physics Abstracts
61.55H — 61.10 — 64.70K

Single crystal X-ray study of a modulated icosahedral AlCuFe phase

N. Menguy (1), M. de Boissieu (1), P. Guyot (1), M. Audier (1), E. Elkaim (2) and J. P. Lauriat (2)

(1) Laboratoire de Thermodynamique et Physico-Chimie Métallurgiques, Domaine Universitaire, B.P. 75, 38402 St Martin d'Hères Cedex, France
(2) LURE/CNRS/CEA/MEN, Bât. 209 D, 91405 Orsay Cedex, France

(*Received 2 February 1993, revised 20 April 1993, accepted 28 May 1993*)

Abstract. — A single grain of a modulated icosahedral AlCuFe phase has been studied by X-ray diffraction using the synchrotron light source at LURE (Laboratoire pour l'Utilisation du Rayonnement Electromagnétique, Orsay, France), Each main icosahedral reflection is flanked by twelve satellites along fivefold directions. The integrated intensity of 22 reflections and of their satellites have been measured in a broad $G_{\parallel}$ and $G_{\perp}$ range. Despite the presence of the satellites the overall icosahedral symmetry is maintained. The results are interpreted on the basis of six independent displacive cosine waves, propagating along the fivefold axes of the 6-dim periodic space. The polarization of these cosine waves is found to be longitudinal with a main component in perpendicular space which means that the modulation is of « phason » origin.

1. Introduction.

In the vicinity of the composition $Al_{63.5}Cu_{24}Fe_{12.5}$ it has been shown that the icosahedral phase is only stable at high temperatures [1, 2]. When slowly cooled from 820 °C, the icosahedral phase undergoes a phase transition towards a crystalline multi-domain structure of a rhombohedral phase ($a_R = 32.18$ Å, $\alpha = 36°$). Domains (of about 200 Å in size) are coherently oriented along each of the 10 possible threefold axes of the icosahedron. They reproduce all together an overall icosahedral symmetry, but with a characteristic splitting of the Bragg reflections. This phase transition is reversible and occurs around 675 °C [2-4].

The icosahedral modulated phase has been discovered as a transient state of this transition. Electron diffraction patterns consist of the Bragg reflections of the icosahedral phase together with satellite reflections surrounding each main peak. This so-called modulated phase was obtained after annealing dodecahedral single grain particles of the icosahedral phase quenched from 820 °C to room temperature. The modulation wavelength varies from 150 Å to 400 Å depending on temperature and annealing time which typically ranges from 450 to 600 °C and from 1 min to a few hours. It has been first postulated that these modulated phase is a transient state between the icosahedral and the rhombohedral phase. However, from recent further TEM

investigations which will be reported elsewhere, we have identified that this modulated icosahedral state first evolves towards a mixture of two pentagonal structures which, in turn, transforms into the rhombohedral one.

The Al-Fe-Cu equilibrium phase diagram has been extensively studied by various groups, in the tiny area where the icosahedral phase forms [5-8]. The composition of the as grown dodecahedral particles, as measured from electron probe micro-analysis, is $Al_{63.5}Cu_{24}Fe_{12.5}$ and fall in so-called « complex » or « approximant » domains [9]. To be noted that the so-called « Debye-Waller phase » studied by Bancel is in fact such a modulated phase [10].

Crystal-quasicrystal phase transitions have also been extensively studied theoretically within a hyperspace description of the icosahedral and approximant phases [11-14]. In the 6-dim description of the i-phase, the « phason » degree of freedom in the perpendicular space $E_\perp$ corresponds to atomic jumps in physical space $E_\parallel$ and are diffusive modes [15-17]. Transitions between the i-state and approximant crystals can result of phasons linearly correlated. Group theory arguments restrict the possible set of phason strain for such transitions [11, 12] (a similar work with phonons has been carried out by Fradkin [13]). In the Landau theory description, stability and phase transitions towards lower symmetry phases (C_5, D_{3h}, C_{2h}) were discussed in terms of phasons or phonons instabilities. In this scheme, a soft phason mode appears as a precursor candidate of the transition, giving rise to diffuse scattering with characteristic shape [18-20]. Such elastic instabilities have also been discussed by Widom [20] and Henley [21, 22] for random tiling models and were introduced by Goldman *et al.* [23], and Bancel [24] to interpret their temperature dependent peak intensity and shape in X-ray diffraction experiments. According to these arguments it would thus be tempting to interpret the modulated phase as resulting from such phason mode softening.

In order to specify the nature of the modulated state, we have carried out a quantitative study of the position and of the integrated intensities of the main and satellites reflections by means of a single modulated i-crystal X-ray diffraction experiment. The results are interpreted in terms of phasons waves.

2. Experimental results.

A dodecahedral particle of perfect i-state was quenched from 820 °C to room temperature and annealed at 600 °C for 1 min 30 s in order to transform the icosahedral state into a modulated icosahedral structure. This particle was ground in spherical shape ($R \approx 100$ μm) and then sticked on the tip of a fine glass rod for X-ray diffraction analysis. From X-ray Laue diffraction pattern, this particle was checked to be single phase and single grain.

Electron diffraction patterns recorded with similar samples have shown that the wavelength of the modulation is of the order of 200 Å, as deduced from their satellites distance, $|\mathbf{q}_\parallel| = 0.03$ Å^{-1}, from all the main reflections. Such a narrow distance in reciprocal space, combined with the fact that satellite intensities are very weak, precludes the use of standard X-ray sources for intensity measurements and naturally leads to the choice of the synchrotron radiation where high flux and high resolution are easily achieved. The experiment was carried out at the synchrotron light source of LURE (Laboratoire d'Utilisation du Rayonnement Electromagnétique, Orsay) on the wiggler line W22. The incident beam energy was tuned with a double monochromator Si(111) and the chosen wavelength was $\lambda = 0.6884$ Å. The crystal-detector distance was 35 cm, with an aperture of 0.3×0.3 mm. This led to a Q resolution almost constant for all directions in reciprocal space and ranging from 2 to 4×10^{-3} Å^{-1}

A typical radial scan, through the $N = 7$, $M = 11$ reflection (using the Cahn, Shechtman, Gratias indexing scheme [25]) along a fivefold axis is shown in figure 1. Around each main reflection, twelve satellites have been measured. They lye along the 6 fivefold directions of an icosahedron centered on the main reflection. As previously observed by electron diffraction,

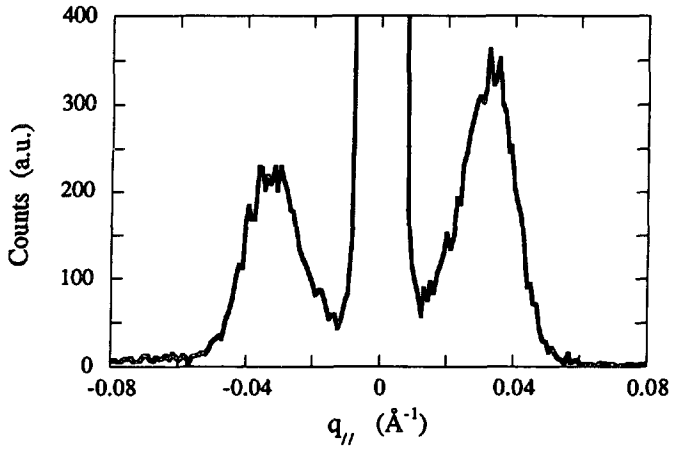

Fig. 1. — Longitudinal scan through the fivefold reflection $N = 7$, $M = 11$.

these satellite reflections have an ellipsoidal shape elongated along the fivefold axes. This is illustrated in figure 2a, where measurements of two longitudinal widths of a satellite can be compared to this of its radial width, which is smaller. Longitudinal and radial widths of satellites (i.e. their full width at half maximum FWHM) are constant for all reflections, equal to 0.02 Å^{-1} and 0.01·Å^{-1} respectively ; the FWHM of the main reflections is smaller (5×10^{-3} Å^{-1}). One should also note that the intensity ratio between satellite and main reflections is about 1/500. Two different configurations of satellites observed around the 3/4 and 6/9 fundamental icosahedral reflections are shown in figure 2b.

Due to the elongated shape of the satellite reflections and to their position close to the fundamental reflection, standard intensity measurement such as ω-scan, are not appropriated. In order to collecte satellite intensities under comparative conditions, all the scans have been carried out following the directions joining the icosahedral reflection to each of their 12 satellites. The sizes of the aperture used in front of the detector were chosen such as an overlap between different satellite reflections was avoided.

Position and integrated intensities have been evaluated by fitting each reflection with a Gaussian profile, using the ABFfit software [26]. A typical result of such a fit is shown figure 3. All satellite reflections were found at a distance $|q_{\parallel}| = 0.031$ Å^{-1} from the main reflection, which corresponds to a modulation wavelength of 200 Å.

The positions of the main reflections do not depart from those of the perfect icosahedral phase. Their widths are also comparable to those measured for a perfect quasicrystalline phase [27] and are independent of $G_{\perp}$, as shown figure 4. This illustrates the high degree of coherency and the quality of the sample.

As it has been observed from similar measurements carried out on a perfect AlCuFe icosahedral phase [5], ω-scans of the main reflections show tails and have a Lorentzian shape. This is probably due to surface damage introduced during the spherical grounding of the dodecahedral particle. This shape is the same at low and large ω, similarly to a mosaic effect. This made difficult the measurement of the satellite intensities near high angle strong reflections.

For the fundamental icosahedral reflections, we have verified that the structure factor, determined from intensities corrected of the mean atomic scattering factor remains similar to the one of the perfect icosahedral phase (Fig. 5) : the variation of the structure factor *versus*

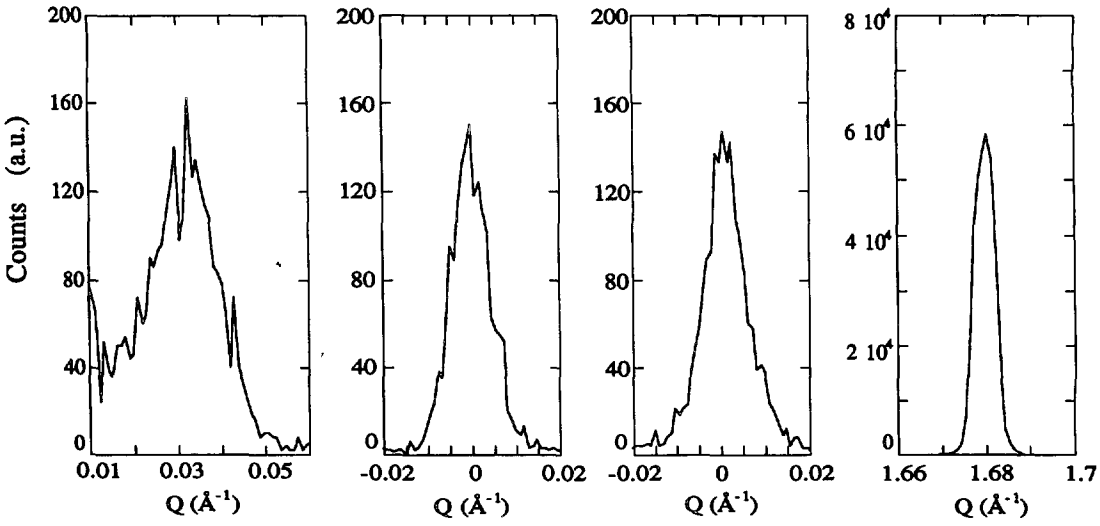

a)

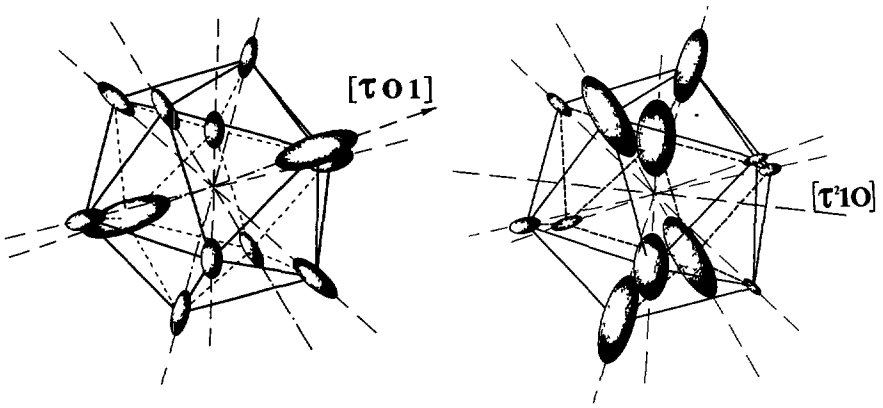

b)

Fig. 2. — a) Intensity distribution of a satellite belonging to the $N = 6$, $M = 9$ main reflection : (from left to right) longitudinal direction (along the fivefold axis), transverse scan (in diffracting plane, ω-scan), transverse scan (out of diffracting plane, χ scan). For comparison the radial scan of the main reflection is shown to the right. b) Illustration of the configuration of satellites surrounding icosahedral reflections located on the fivefold axis $[\tau 01]$ $(N/M = 3/4)$ and threefold axis $[\tau^2 10](N/M = 6/9)$. Ellipsoids represent the reflection shapes ; their size are proportional to their intensities (these representations are related to results shown in Fig. 6).

$G_\perp$ occur along four branches depending on the N, M parity rules. Despite the small number of studied reflections (22 fundamental reflections, in broad $G_\parallel$ (0.7 to 8 $Å^{-1}$) and $G_\perp$ (0.1 to 0.7 $Å^{-1}$) ranges), our results appear to be in good agreement with those shown in reference [27] for the perfect i-phase. It can thus be pointed out that the atomic surfaces remain almost unmodified during the icosahedral → modulated icosahedral transition.

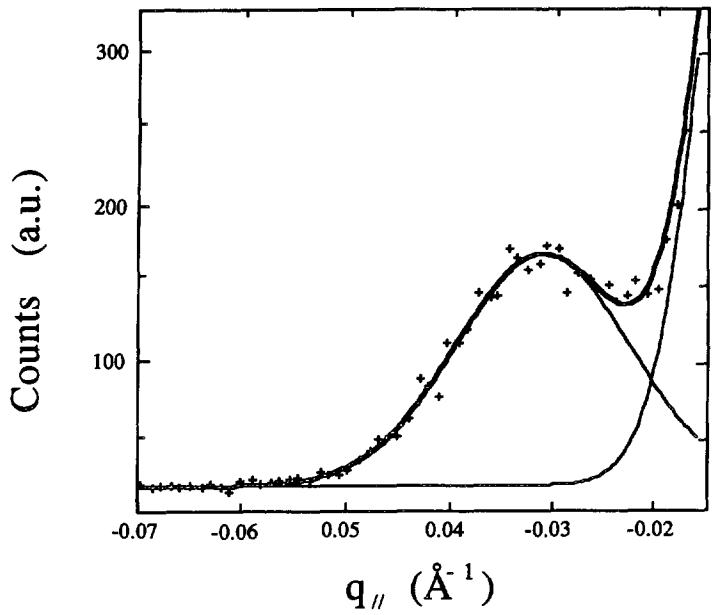

Fig. 3. — Typical result of a Gaussian fit of a satellite. The bottom part of the main peak is also fitted with a Gaussian.

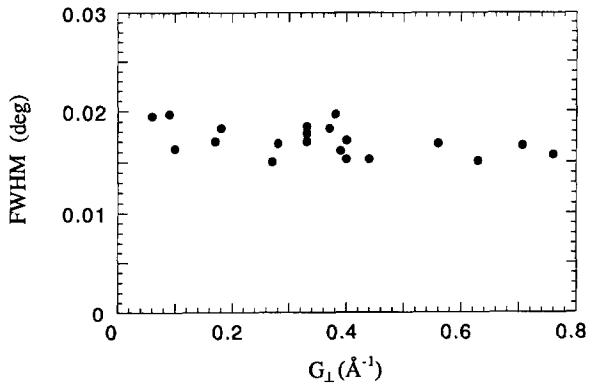

Fig. 4. — FWHM of the main reflections *versus* $G_\perp$.

In order to evidence the possible phonon or phason contributions to the modulation, the intensities of the satellites surrounding these 22 icosahedral reflections have been measured.

The figure 6 shows the 12 satellite intensities measured around different types of main reflections located successively on fivefold, threefold and twofold symmetry axes. It appears that important satellite intensity variations are clearly correlated to the symmetry of the main reflection (see also Fig. 2b) :

(i) around a reflection on a fivefold axis, there are two strong satellites, colinear with the fivefold axis, and ten weaker reflections (Fig. 6a) ; these ten satellites have the same intensity and correspond to five equivalent fivefold directions with respect to $\mathbf{G}_\parallel$;

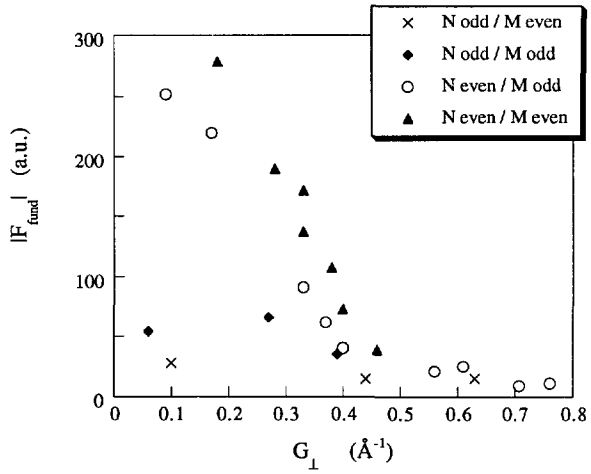

Fig. 5. — Structure factor of the main Bragg reflections. The measured integrated intensity has been corrected by different terms (Lorentz, absorption, Debye-Waller) and normalized by a $\langle f_i^2 \rangle$ to account for the q dependence of the X-ray atomic form factor.

(ii) similarly it can be shown that for threefold reflections, the satellites fall into two groups (6, 6) (Fig. 6b) ;

(iii) for twofold reflections there are three groups (4, 4, 4) (Fig. 6c).

It was thus checked that the integrated intensity of all measured satellites remain in agreement with the icosahedral symmetry or, in other words that the overall icosahedral symmetry is not broken by the modulation phenomenon. Using the results of figure 6, one evidences a strong correlation between the sum of the amplitudes of the satellites of a pair at $(\mathbf{G}^j_\perp \pm \mathbf{q}^j_\parallel)$ with cos $(\mathbf{G}^j_\perp ; \mathbf{q}^j_\perp)$ (Fig. 7). $\mathbf{q}^j_\parallel$ **and** $\mathbf{q}^j_\perp$ are the components in parallel and perpendicular spaces of the modulation wave vector $\mathbf{q}^j$. $\mathbf{q}^j_\perp$ is assumed to lye along a j fivefold direction (see after).

As previously observed by electron diffraction, the intensity of the satellite at + $\mathbf{q}_\parallel$ from the main reflection is, in general, different from the one at – $\mathbf{q}_\parallel$ [28]. This asymmetry is correlated to the sign of $\mathbf{G}_\perp$, as also noticed by Bancel [8] on powder samples. This is best exemplified when looking at strong satellite intensities around fivefold Bragg reflections (i.e. for a longitudinal scan) : the figure 8a shows a serie of systematic reflections which are in a τ scaling in the parallel space (2/1, 3/4, 7/11, 18/29). To the τ inflation in the parallel space corresponds a $-\tau^{-1}$ deflation in the perpendicular space and thus an alternate change of sign of $\mathbf{G}_\perp$ (Fig. 8b). Reflections with the same sign of $\mathbf{G}_\perp$ (2/1 and 7/11) have the same type of intensity asymmetry, whereas for the opposite sign of $\mathbf{G}_\perp$, the intensity asymmetry is reversed (3/4 and 18/29).

These two characteristics of the satellites, scaling with cos $(\mathbf{G}^j_\perp ; \mathbf{q}^j_\perp)$ and the sign of the asymmetry, can be interpreted as resulting from strain waves with wave vectors lying along the fivefold j axes of the structure with a predominant longitudinal phason component, as now discussed.

3. Discussion.

In a first approach, the modulation can be assumed to be the result of a superimposition of six equivalent independent cosine waves straining the i-crystal. If the modulated phase is related

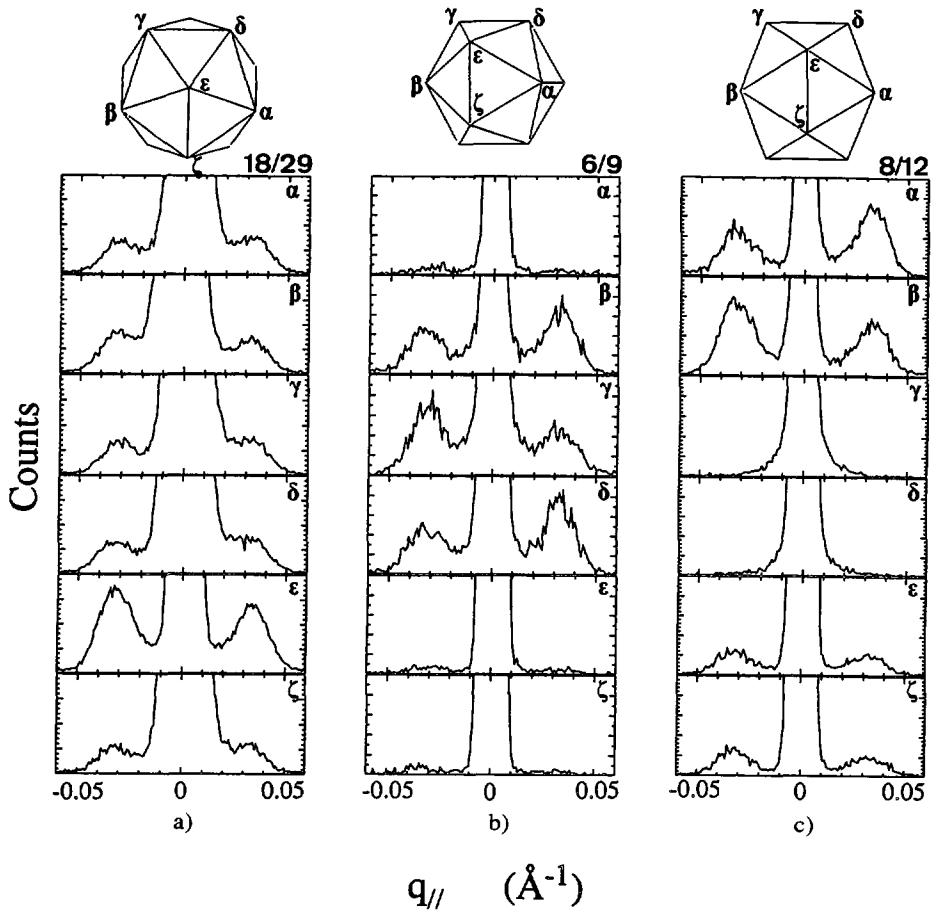

Fig. 6. — Satellites reflections measured around icosahedral Bragg peaks of fivefold, threefold and twofold symmetry. The intensity of satellites depends on their relative position with respect to the main one : (from the left to the right) « fivefold » satellites are gathered in 2 groups (2-10 satellites), « threefold » in 2 groups (6-6 satellites) and twofold in 3 groups (4-4-4).

somehow to the transition from the icosahedral to the rhombohedral phase, phasons are supposed to play a major role. This implies that the strain field involving *a priori* six degrees of freedom for phasons and phonons, has to be done in the 6-dim periodic space.

As selected area electron diffraction patterns, where the diffracting area has a diameter of the order of 150 nm, and X-ray diffraction patterns look very similar, our results show that even at such a small scale the 6 strain waves coexist in the same part of the sample. Further, recent Fourier transform analyses of high resolution TEM micrographs of this modulated i-structure, oriented along a twofold zone axis, have confirmed the existence of two pairs of satellites for selected area diameters down to 40 nm [29]. Therefore the modulated structure seems to be homogeneous at this scale, ruling out the association of one domain to a single strain wave.

The simulation of the satellite intensities may be carried out in a way very similar to what is done for 3-dim displacive modulated structures. We start with a i-structure described by a set of atomic surfaces decorating the 6-dim periodic structure. If atomic surfaces lye in

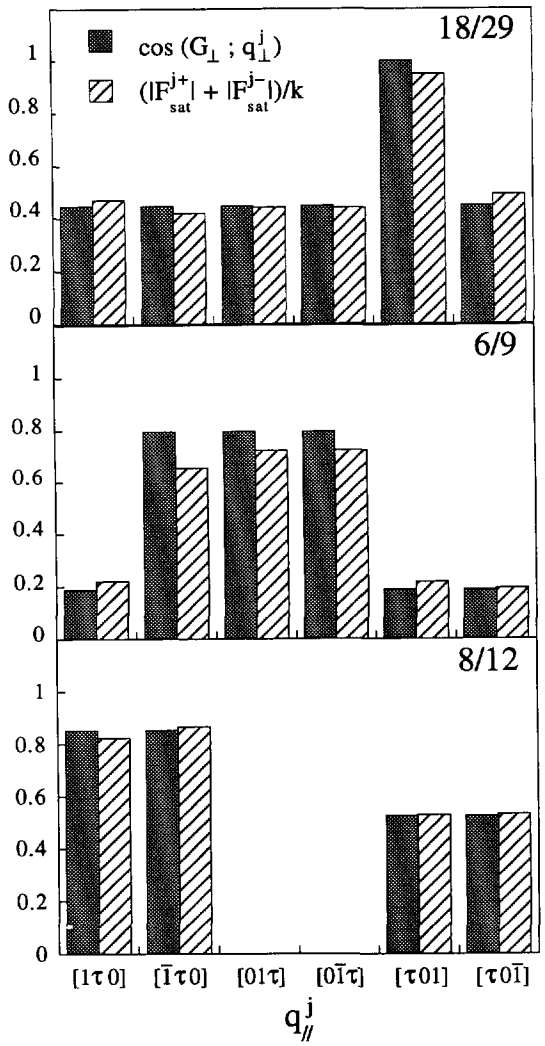

Fig. 7. — Correlation between the sum of the amplitudes of the satellites of a pair at $\mathbf{G}_{\parallel} \pm \mathbf{q}^{j}_{\parallel}$ and $\cos(\mathbf{G}_{\perp}, \mathbf{q}^{j}_{\perp})$. For this plot, the sum of the amplitudes have been divided by a factor k defined as :

$$k = \frac{1}{6} \sum_{j=1}^{6} \frac{[F^{j+}_{sat}(\mathbf{G}_{\parallel}) + F^{j-}_{sat}(\mathbf{G}_{\parallel})]}{\cos(\mathbf{G}_{\perp}, \mathbf{q}^{j}_{\perp})}$$

perpendicular space the scattering amplitude at the point of reciprocal space $\mathbf{G}_{\parallel}$ is given by :

$$F(\mathbf{G}_{6D}) = F(\mathbf{G}_{\parallel} ; \mathbf{G}_{\perp}) = \sum_{6\text{-cube}} e^{i\mathbf{G}_{6D} \cdot \mathbf{r}_i} \Omega_i^*(\mathbf{G}_{\perp}) f_i(\mathbf{G}_{\parallel}) \quad (1)$$

where $\Omega_i^*(\mathbf{G}_{\perp})$ is the Fourier transform of the atomic surface i, located at $\mathbf{r}_i$ in the 6-dim cube unit cell and f_i the atomic scattering amplitude of the specie i.

We then deform this lattice, with 6 cosine waves of wavevector $\mathbf{q}^{j}_{6D} = (\mathbf{q}^{j}_{\parallel}, \mathbf{q}^{j}_{\perp})$ and a polarization $\mathbf{U}^{j}_{6D} = (\mathbf{U}^{j}_{\parallel}, \mathbf{U}^{j}_{\perp})$. Each atom at $\mathbf{r}_{6D}$ is displaced of :

$$\mathbf{U}_{6D}(\mathbf{r}_{6D}) = \sum_{j=1}^{6} \mathbf{U}^{j}_{6D} \cos(\mathbf{q}^{j}_{6D} \cdot \mathbf{r}_{6D}) = \sum_{j=1}^{6} (\mathbf{U}^{j}_{\parallel} + \mathbf{U}^{j}_{\perp}) \cos(\mathbf{q}^{j}_{\parallel} \cdot \mathbf{r}_{\parallel} + \mathbf{q}^{j}_{\perp} \cdot \mathbf{r}_{\perp}). \quad (2)$$

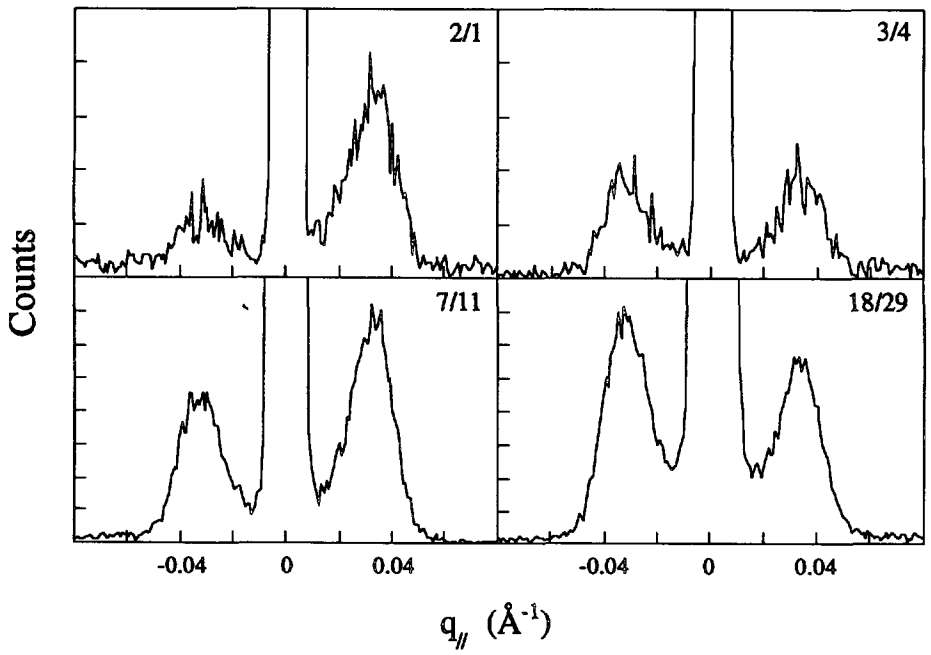

a)

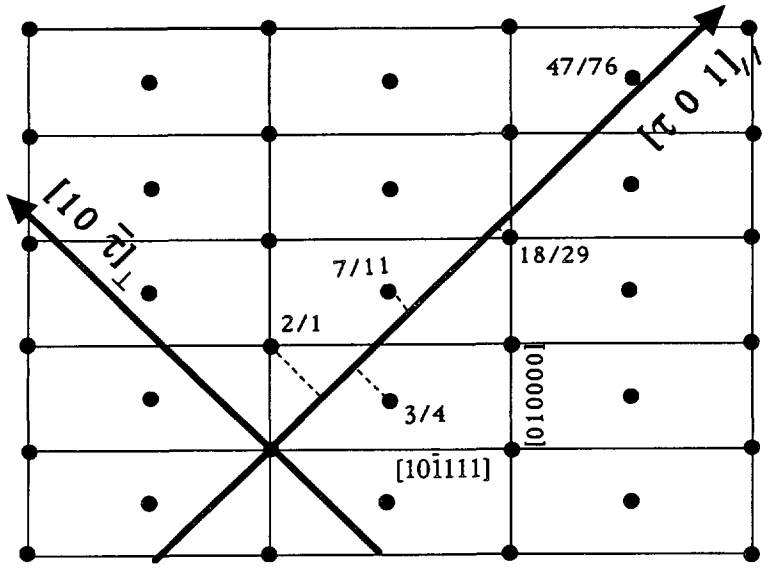

b)

Fig. 8. — a) Illustration of the correlation between the asymmetry for satellites at + **q** and − **q** with the sign of $\mathbf{G}_{\perp}$ of the main reflection. Reflections 2/1, 3/4, 7/11 and 18/29 along a fivefold axis are in a τ inflation sequence, with a change of the $\mathbf{G}_{\perp}$ sign at each step. b) Rational cut of the 6-dim reciprocal space in a plane containing two fivefold directions, both in physical and perpendicular spaces respectively. The observed reflections are labelled with the N and M indices.

The parallel $\mathbf{U}_\parallel$ and perpendicular $\mathbf{U}_\perp$ components of this displacement field correspond to phonon and phason components respectively. It is easy to show that the Fourier transform of such a deformed quasicrystal gives Bragg peaks at the fundamental $\mathbf{G}_\parallel$ reflections of the undeformed quasicrystal, with the structure factor :

$$F_{\text{fund}}(\mathbf{G}_\parallel) = F(\mathbf{G}_{6D})\, J_0[\mathbf{G}_{6D} \cdot \mathbf{U}_{6D}] \tag{3}$$

where $F(\mathbf{G}_{6D})$ is given by equation (1) and J_0 is the Bessel function of 0-th order. Each of them is flanked by $6 \times 2\,n$ satellites of structure factor :

$$F^{nj}_{\text{sat}}(\mathbf{G}_\parallel \pm n\mathbf{q}'_\parallel) = F(\mathbf{G}_{6D} \pm n\mathbf{q}'_{6D})\, J_n((\mathbf{G}_{6D} \pm n\mathbf{q}'_{6D}) \cdot \mathbf{U}^j_{6D}) \tag{4}$$

where J_n is the Bessel function of n-th order. If the amplitude of the modulation is small, the first order satellite, in the direction $\mathbf{q}'_\parallel$, has an amplitude given by :

$$F^j_{\text{sat}}(\mathbf{G}_\parallel \pm \mathbf{q}'_\parallel) = \frac{1}{2} F(\mathbf{G}_{6D} \pm \mathbf{q}'_{6D})\, (\mathbf{G}_{6D} \pm \mathbf{q}'_{6D}) \cdot \mathbf{U}^j_{6D} \tag{5}$$

$$= \frac{1}{2} F(\mathbf{G}_{6D} \pm \mathbf{q}'_{6D})\, [(\mathbf{G}_\parallel \pm \mathbf{q}'_\parallel) \cdot \mathbf{U}^j_\parallel + (\mathbf{G}_\perp \pm \mathbf{q}'_\perp) \cdot \mathbf{U}^j_\perp]\,. \tag{6}$$

Then, to first order, the sum of the amplitudes of two satellites aligned in the direction $\mathbf{q}'_\parallel$ for a given reflection $\mathbf{G}_\parallel$ is :

$$[F^{j+}_{\text{sat}}(\mathbf{G}_\parallel) + F^{j-}_{\text{sat}}(\mathbf{G}_\parallel)] = F_{\text{fund}} \cdot [\mathbf{G}_\parallel \cdot \mathbf{U}^j_\parallel + \mathbf{G}_\perp \cdot \mathbf{U}^j_\perp]\,. \tag{7}$$

From diffraction data, only the parallel component $\mathbf{q}'_\parallel$ of the modulation wavevector is measured, and its $\mathbf{q}'_\perp$ counterpart is unknown. We assume further than $\mathbf{q}'_{6D}$ stands along a five-fold axis of 6D space, for instance $\mathbf{q}_{6D}$ lye along $\langle 10\bar{1}111\rangle$ or $\langle 010000\rangle$ on the cut of 6D space of figure 8b. Then $\mathbf{q}'_\perp$ stands also along a fivefold axis in $E_\perp$ and $|\mathbf{q}'_\perp| = |\mathbf{q}'_\parallel|$ ($\mathbf{q}'_\perp$ and $\mathbf{q}'_\parallel$ lye respectively along $\langle 10\,\bar{\tau}\rangle_\perp$ and $\langle \tau 01\rangle_\parallel$ in Fig. 8b).

This model allows us to explain the asymmetry between satellite reflections at $+\mathbf{q}'_\parallel$ and $-\mathbf{q}'_\parallel$. For all measured satellites, $|\mathbf{G}_\perp|$ varies from 0.1 to 0.7 Å^{-1} ; compared to the value of $|\mathbf{q}'_\perp| = 0.03$ Å^{-1}, $|\mathbf{q}'_\perp|$ is not negligible in front of $|\mathbf{G}_\perp|$ and is therefore responsible of the asymmetry between satellite reflection intensities. It originates from two different terms of expression (6) which can vary oppositely :

(i) from the scalar product $\mathbf{U}^j_\perp \cdot (\mathbf{G}_\perp \pm \mathbf{q}'_\perp)$, the satellite intensity at $\mathbf{q}'_\parallel$ will be stronger than the one at $-\mathbf{q}'_\parallel$ when $\mathbf{G}_\perp$ and $\mathbf{q}'_\perp$ have the same sign (e.g. case of 2/1 reflection) and the opposite for opposite sense between $\mathbf{G}_\perp$ and $\mathbf{q}'_\perp$ (e.g. case of 18/29 reflection) ;

(ii) from the term $F(\mathbf{G}_{6D} \pm \mathbf{q}'_{6D})$ related to the Fourier transforms of atomic surfaces $\Omega_i{}^*$ which correspond to oscillating functions which tend to zero at large $|\mathbf{G}_\perp|$ values (Fig. 5), it appears that for small $|\mathbf{G}_\perp|$ values, $\Omega^*(\mathbf{G}_\perp + \mathbf{q}'_\perp)$ will be smaller than $\Omega^*(\mathbf{G}_\perp - \mathbf{q}'_\perp)$ if $\mathbf{G}_\perp$ and $\mathbf{q}'_\perp$ have the same sign (and respectively larger if $\mathbf{G}_\perp$ and $\mathbf{q}'_\perp$ have opposite signs).

The polarization $\mathbf{U}^j_{6D}$ has been found to be essentially of phason origin and « longitudinal », i.e. $\mathbf{U}^j_{6D} \approx \mathbf{U}^j_\perp$ and parallel to the $\mathbf{q}'_\perp$ vector. This can be infered qualitatively from the correlation between the sum of the amplitudes of satellites which are aligned in the direction $\mathbf{q}'_\parallel$, and $\cos(\mathbf{G}'_\perp, \mathbf{q}'_\perp)$ of figures 6 and 7 and quantitatively from the linear variation of $(F^{j+}_{\text{sat}} + F^{j-}_{\text{sat}})/F_{\text{fund}}$ as a function of the scalar product $\mathbf{G}_\perp \cdot \mathbf{U}^j_\perp$. $\mathbf{G}_\perp \cdot \mathbf{U}^j_\perp = |\mathbf{G}_\perp| \cdot |\mathbf{U}^j_\perp| \cos(\mathbf{G}_\perp ; \mathbf{q}'_\perp)$ (Fig. 9a). From equation (7) this shows that the modulation results essentially from phason waves : with the same plot, done as a function of

$\mathbf{G}_{\parallel} \cdot \mathbf{U}_{\parallel}^{j}$ (with $\mathbf{U}_{\parallel}^{j}$ along a fivefold axis and parallel to $\mathbf{q}_{\parallel}^{j}$) there is no correlation (Fig. 9b). This proves that the phonon contribution to the modulation is negligible with respect to the phason one. If not, the plot of figure 9a could not be linear. The amplitude of the modulation $|\mathbf{U}_{\perp}^{j}|$ can then be deduced from the slope of the straight line obtained from a linear regression of the figure 9a : $|\mathbf{U}_{\perp}^{j}|$ is found equal to 0.35 Å ([1]).

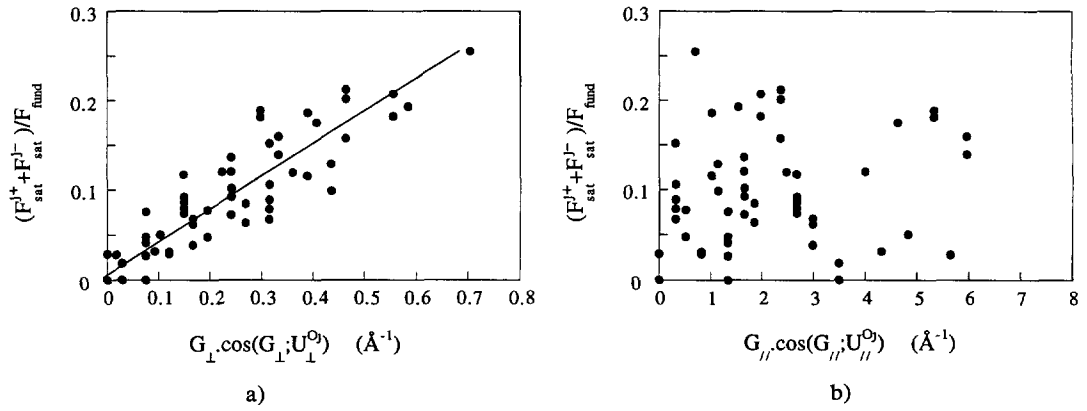

Fig. 9. — a) $G_{\perp}$ dependence of the ratio $(F_{sat}^{j+} + F_{sat}^{j-})/F_{fund}$ for all measured satellite reflections. b) Same plot as in (a) as a function of $G_{\parallel}$.

In order to attempt a refinement of this modulated structure from experimental data, we introduce in the approach a model of the atomic structure of the i-AlFeCu phase. Following what has been carried out in the case of the i-AlPdMn phase, which is isostructural to AlCuFe [30], the different atomic surfaces have been modelized with spheres. Such an approximation is justified by the low values of $|\mathbf{G}_{\perp}|$ ($|\mathbf{G}_{\perp}| < 0.7$ Å^{-1}) corresponding to the measured reflections. In this range of $|\mathbf{G}_{\perp}|$ the value of $\Omega^*(\mathbf{G}_{\perp})$ depends mainly on the volume of the atomic surface and not on its precise shape ; effectively the $|\mathbf{G}_{\perp}|$ dependence of the main reflections show a smooth behaviour (Fig. 5). Then taking into account the models proposed for *F*-icosahedral AlCuFe [27] and AlPdMn [30] the following atomic surfaces were used :

(i) on even node : a sphere of iron with a radius $R = 0.8\ a_{6D}$, enclosed in a sphere of copper with radius $R = 1.34\ a_{6D}$ and a final shell of aluminum with radius $R = 1.52\ a_{6D}$. a_{6D} is the 6-dim cube parameter, equal to 6.317 Å ;

(ii) on odd node : an iron sphere with a radius $R = 0.78\ a_{6D}$, and an Al shell with radius $R = 1.64\ a_{6D}$;

(iii) on odd body centre, a sphere of copper with radius $R = 0.71\ a_{6D}$.

This model gives a reasonable agreement when compared with data (*R* factor of the order of 0.11, (see Tab. I)).

The intensities of the fundamental and satellite reflections have been calculated according to equations (1) and (6), with in a first step, $\mathbf{U}_{\parallel} = 0$. We keep, as previously, $\mathbf{U}_{\perp}^{j}$ parallel to $\mathbf{q}_{\perp}^{j}$ and $|\mathbf{q}_{\perp}^{j}| = 0.03$ Å^{-1} The best fit obtained from 60 independent pairs of satellite

([1]) This value differs from the value published in the proceedings of the Fourth International Conference on Quasicrystals of St Louis, 1992 [31] and which is 2 π too large, due to an error in the length of reciprocal space vectors.

Table I. — *Comparison between the measured intensities of the icosahedral reflections and those calculated from a simple 6-dim structural model. (*) The measured intensities have corrected by the Lorentz, absorption and Debye-Waller factors.*

Indices N/M	Indices h/h' k/k' l/l'	Multiplicity	$G_{//}$ ($Å^{-1}$)	$G_{\perp}$ ($Å^{-1}$)	Measured intensity *	Calculated intensity
2/1	0/1 0/0 1/0	12	0.704	0.704	250	1300
3/4	1/1 0/0 0/1	12	1.139	0.438	630	100
6/9	1/2 0/1 0/0	20	1.679	0.398	3820	2820
7/11	1/2 0/0 1/1	12	1.843	0.269	9760	6410
8/12	2/2 0/0 0/0	30	1.938	0.458	3280	2520
11/16	1/3 0/0 0/1	60	2.248	0.627	460	940
14/21	2/3 0/0 1/0	60	2.564	0.607	1120	1460
18/29	2/3 0/0 1/2	12	2.982	0.169	75080	72700
20/32	2/4 0/0 0/0	30	3.137	0.279	53360	41000
22/33	2/4 1/0 0/1	120	3.214	0.757	170	240
27/43	3/4 0/0 1/1	60	3.637	0.388	1560	1485
38/61	3/5 1/1 1/1	60	4.328	0.329	8100	6000
40/64	3/5 0/1 1/2	60	4.435	0.398	4950	3775
46/73	3/6 0/1 0/0	60	4.742	0.557	390	498
47/76	3/5 0/0 2/3	12	4.826	0.099	650	125
52/84	4/6 0/0 0/0	30	5.074	0.179	57060	39320
72/116	4/6 0/0 2/4	12	5.966	0.329	14970	5530
72/116	4/7 1/2 1/1	60	5.966	0.329	9620	5530
90/145	4/7 0/0 3/4	12	6.67	0.368	1430	680
102/165	5/8 2/3 0/0	20	7.111	0.089	19580	13800
123/199	5/8 0/0 3/5	12	7.809	0.059	660	485
124/200	6/9 1/2 1/1	120	7.832	0.378	2590	835

reflection intensities lead to a value $|\mathbf{U}'_{\perp}| = 0.25$ Å and to a R factor equal to 0.35. The value of $|\mathbf{U}'_{\perp}|$ appears therefore to be consistent with the value previously obtained from the direct analysis of the diffraction data. This model also shows that the asymmetry of the satellite intensity originating mainly from the term $\Omega^*(\mathbf{G}_{\perp} \pm \mathbf{q}'_{\perp})$ can be quite large, especially when $\Omega^*(\mathbf{G}_{\perp})$ is close to zero. Results of the fit are gathered in table II. Introducing a $\mathbf{U}_{\parallel}$ parallel component in this simulation leads to a $|\mathbf{U}_{\parallel}|$ value of one order of magnitude lower than $|\mathbf{U}'_{\perp}|$, without modifying the reliability factor R.

Conclusion.

The single crystal X-ray diffraction study of the modulated icosahedral phase shows that the presence of satellite reflections does not destroy the icosahedral symmetry of the diffraction pattern. It has been checked that not only the position of the Bragg reflections (mains and satellites reflections) but also their integrated intensity fulfill the icosahedral point group symmetry. Sixty independent pairs of satellite reflections have been measured. Results can be interpreted by the superimposition of six cosine strain waves, propagating along the six $\langle 100000 \rangle$ directions of the 6-dim lattice. The polarization vectors have mainly a perpendicular component $\mathbf{U}'_{\perp}$ parallel to the six fivefold axes in the perpendicular space and are therefore longitudinal. This simple model allows us to explain fairly well our experimental results. The

Table II. — *Comparison between the measured and calculated satellite reflections intensities : average intensities of equivalent pairs of satellites are reported for N/M icosahedral reflections of different multiplicities.* α *is the angle between* $\mathbf{G}_\perp$ *and* $\mathbf{q}'_\perp$ *. N.B.* I_{meas} *have been corrected by different terms as in table I.*

REFLECTIONS WITH A MULTIPLICITY EQUAL TO 12

N/M	$\lvert\cos\alpha\rvert = 1$		$\lvert\cos\alpha\rvert \approx 0.447$	
	$I_{meas.}$	$I_{calc.}$	$I_{meas.}$	$I_{calc.}$
2/1	0.51	12.9	0.276	1.9
	1.92	6.34	0.288	1.89
3/4	1.63	0.73	0.305	0.021
	1.45	0.04	0.426	0.111
7/11	15.7	12.9	2.58	4.37
	23.9	15.8	3.02	1.69
18/29	88.2	83	31.6	5.32
	69.4	59	39.7	26.9
47/76	2.13	0.016	0	0
	0	0.019		
72/116	139	29	44.3	5.91
	80.8	49.7	50.1	9.26
90/145	26.7	6.71		
	41.8	1.46		
123/199	0	0.25		
	0	0.030		

REFLECTIONS WITH A MULTIPLICITY EQUAL TO 20

N/M	$\lvert\cos\alpha\rvert \approx 0.188$		$\lvert\cos\alpha\rvert \approx 0.795$	
	$I_{meas.}$	$I_{calc.}$	$I_{meas.}$	$I_{calc.}$
6/9	0.906	0.207	6.41	16.6
	0.535	0.81	9.3	3.62
102/165	8.19	3.12		
	5.75	0.261		

REFLECTIONS WITH A MULTIPLICITY EQUAL TO 30

N/M	$\lvert\cos\alpha\rvert \approx 0.851$		$\lvert\cos\alpha\rvert = 0$		$\lvert\cos\alpha\rvert \approx 0.526$	
	$I_{meas.}$	$I_{calc.}$	$I_{meas.}$	$I_{calc.}$	$I_{meas.}$	$I_{calc.}$
8/12	14	10.6	0	0.04	4.8	2.77
	8.72	2.82	0	0.04	4.07	1.7
20/32	107	78.1	19.4	1.43	82.4	38.5
	147	83.4	31.5	3.54	80.3	23.5
52/84	148	35	33.1	2.19	16	8.1
	151	59.3	17.5	1.86	23.1	29.7

Table II *(continued).*

REFLECTIONS WITH A MULTIPLICITY EQUAL TO 60

N/M	$I_{meas.}$	$I_{calc.}$	$I_{meas.}$	$I_{calc.}$	$I_{meas.}$	$I_{calc.}$	$I_{meas.}$	$I_{calc.}$
11/16	$\|\cos\alpha\| \approx 0.689$		$\|\cos\alpha\| \approx 0.308$		$\|\cos\alpha\| \approx 0.073$		$\|\cos\alpha\| \approx 0.925$	
	1.86	2.34	0.56	0.40	0	0.09	3.59	4.24
	2.1	3.47	0.92	0.80	0	0.002	5.36	6.06
14/21	$\|\cos\alpha\| \approx 0.123$		$\|\cos\alpha\| \approx 0.520$		$\|\cos\alpha\| \approx 0.766$		$\|\cos\alpha\| \approx 0.918$	
	0	0.56	3.14	5.87	6.32	8.85	11.4	16.3
	0	0.10	3.69	3.9	8.96	11.8	8.91	12.8
27/43	$\|\cos\alpha\| \approx 0.689$		$\|\cos\alpha\| \approx 0.308$		$\|\cos\alpha\| \approx 0.073$		$\|\cos\alpha\| \approx 0.924$	
	4.18	4.24	1.1	0.5	0	0.22	7.92	6.66
	2.91	3.96	0.66	0			5.34	8.19
38/61	$\|\cos\alpha\| \approx 0.227$		$\|\cos\alpha\| \approx 0.960$		$\|\cos\alpha\| \approx 0.680$		$\|\cos\alpha\| \approx 0.507$	
	7.52	0.59	67.5	17.2	33	14.7	11.25	7.64
	4.08	2.6	48.2	37.8	38.4	11.3	11.66	6.63
40/64	$\|\cos\alpha\| \approx 0.602$		$\|\cos\alpha\| \approx 0.973$		$\|\cos\alpha\| \approx 0.230$		$\|\cos\alpha\| \approx 0.372$	
	17.3	8.31	44.1	39.5	0	2.23	8.61	2.95
	14.7	10.8	65.4	15.2			12.94	4.27
46/73	$\|\cos\alpha\| \approx 0.823$		$\|\cos\alpha\| \approx 0.132$		$\|\cos\alpha\| \approx 0.723$		$\|\cos\alpha\| \approx 0.295$	
	6.69	3.64	0	0.02	3.98	2.83		
	4.17	1.87	0	0.15	4.11	1.47		
72/116	$\|\cos\alpha\| = 0$		$\|\cos\alpha\| \approx 0.723$		$\|\cos\alpha\| \approx 0.276$		$\|\cos\alpha\| \approx 0.894$	
	0	2.36	57.6	9.3	11.3	0.18	113	18.6
	0	0.738	46.5	10.7			144	12.509

REFLECTIONS WITH A MULTIPLICITY EQUAL TO 120

N/M	$I_{meas.}$	$I_{calc.}$	$I_{meas.}$	$I_{calc.}$	$I_{meas.}$	$I_{calc.}$	$I_{meas.}$	$I_{calc.}$	$I_{meas.}$	$I_{calc.}$	$I_{meas.}$	$I_{calc.}$
22/33	$\|\cos\alpha\| \approx 0.732$		$\|\cos\alpha\| \approx 0.097$		$\|\cos\alpha\| \approx 0.928$		$\|\cos\alpha\| \approx 0.414$		$\|\cos\alpha\| \approx 0.219$		$\|\cos\alpha\| \approx 0.611$	
	1.63	0.84	0	0.05	2.14	3.55			0.453	0.15	0.60	0.46
	2.66	1.93	0	0.01	4.48	1.1			0.11	0.06	1.09	0.25
124/200	$\|\cos\alpha\| \approx 0.792$		$\|\cos\alpha\| \approx 0.395$		$\|\cos\alpha\| \approx 0.640$		$\|\cos\alpha\| = 0$		$\|\cos\alpha\| \approx 0.151$		$\|\cos\alpha\| \approx 0.885$	
	35.1	6.06	16.4	1.45	28.9	2.8					7.44	0.84
	50.5	3.73	18.9	0.93	19.7	3.47					5.37	1.57

amplitude of the phason modulation is found to be equal to 0.35 Å. This has to be compared to the average size of the atomic surfaces of the order of 10 Å. At this scale, the deformation is small, but this one evolves probably as a function of temperature and time of annealing treatments before the occurrence of a transformation into a mixed state of pentagonal structures. The proposed model also gives some clue about the origin of the asymmetry which is observed between satellites reflections at $+ \mathbf{q}_{\parallel}$ and $- \mathbf{q}_{\parallel}$ around the fundamental reflections : it comes from the perpendicular component of the wave vector. This result may be surprising, since one would expect that the wave has only a parallel component (i.e. in physical space)

where physical properties take place. A further debate on the physical reasons of this modulation phenomenon could be therefore opened.

Note : after submitting this paper, two articles related to studies of modulated icosahedral phases were published respectively by Dénoyer *et al.* [32] and Bancel [33].

References

[1] Audier M. and Guyot P., Quasicrystals and Incommensurate Structures in Condensed Matter, Proceedings of the Third International Meeting on Quasicrystals (Vista Hermosa, Mexico), M. J. Yacaman, D. Romeu, V. Castano, A. Gomez Eds. (1989) p. 288.

[2] Audier M. and Guyot P., Proceedings of the Anniversary Adriatic Research Conference on Quasicrystals (Trieste, Italy), M. V. Jaric and S. Lundqvist Eds. (World Scientific, 1990) p. 74.

[3] Janot C., Audier M., de Boissieu M. and Dubois J. M., *Europhys. Lett.* **14** (1991) 355.

[4] Audier M., Bréchet Y., de Boissieu M., Guyot P., Janot C. and Dubois J. M., *Philos. Mag. B* **63** (1991) 1375.

[5] Bessière M., Quivy A., Lefebvre S., Devaud-Rzepski J. and Calvayrac Y., *J. Phys I France* **1** (1991) 1823.

[6] Faudot F., Quivy A., Calvayrac Y., Gratias D. and Harmelin M., *Mat. Sci. Eng. A* **133** (1991) 383.

[7] Gayle F. W., Shapiro A. J., Biancaniello F. S. and Boettinger W. J., *Metall. Trans. A* **23** (1992) 2409.

[8] Bancel P., Quasicrystals : the State of the Art, D. P. Di Vicenzo and P. Steinhardt Eds. (World Scientific, Singapore, 1991) p. 17.

[9] Gratias D., Calvayrac Y., Devaud-Rzepski J., Faudot F., Harmelin M., Quivy A. and Bancel P., *J. Non-Cryst. Solids* **153 & 154** (1993) 482.

[10] Bancel P. A., Private Communication, 1992.

[11] Ishii Y., *Phys. Rev.* **B 39** (1989) 11862.

[12] Ishii Y., *Philos. Mag. Lett.* **62** (1990) 393.

[13] Fradkin, *JETP Lett.* **51** (1990) 32.

[14] Janssen T., *Europhys. Lett.* **14** (1991) 131.

[15] Kalugin P. A., Kitaev A. Y. and Levitov L. S., *J. Phys. France Lett.* **46** (1985) L601.

[16] Bak P., *Phys. Rev. Lett.* **54** (1985) 1517.

[17] Levine D., Lubensky T. C., Ostlund S., Ramaswamy S., Steinhart P. J. and Toner J., *Phys. Rev. Lett.* **54** (1985) 1520.

[18] Ishii Y., *Phys. Rev.* **B 45** (1992) 5228.

[19] Jaric M. and Nelson R., *Phys. Rev.* **B 59** (1988) 4458.

[20] Widom, Preprint.

[21] Henley C. L., Quasicrystals and Incommensurate Structures in Condensed Matter, Proceedings of the Third International Meeting on Quasicrystals (Vista Hermosa, Mexico), M. J. Yacaman, D. Romeu, V. Castano, A. Gomez Eds. (1989) p. 152.

[22] Henley C. L., Quasicrystals : the state of the art., D. P. Di Vincenzo and P. J. Steinhardt Eds. (World Scientific, 1991) p. 429.

[23] Goldman A. I., Shield J. E., Guryan C. A. and Stephens P. W., Proceedings of the Anniversary Adriatic Research Conference on Quasicrystals (Trieste, Italy), M. V. Jaric and S. Lundqvist Eds. (World Scientific, 1990) p. 60.

[24] Bancel P. A., *Phys. Rev Lett.* **63** (1989) 2741.

[25] Cahn J. W., Shechtman D. and Gratias D., *J. Mat. Res.* **1** (1986) 13.

[26] Antionadis A., Berruyer J. and Filhol A., Affinement de spectres de diffraction de poudre par la méthode du maximum de vraisemblance (I.L.L., 1990).

[27] Cornier-Quiquandon M., Quivy M., Lefebvre S., Elkaim E., Heger G., Katz A. and Gratias D., *Phys. Rev B* **44** (1991) 2071.

[28] Menguy N., Audier M. and Guyot P., *Philos. Mag. Lett.* **65** (1992) 7.
[29] Menguy N., Thesis I.N.P. Grenoble (1993).
[30] Boudard M., de Boissieu M., Janot C., Dubois J. M. and Dong C., *Philos. Mag. Lett.* **64** (1991) 197.
[31] Menguy N., de Boissieu M., Guyot P., Audier M., Elkaim E. and Lauriat J. P., *J. Non-Cryst. Solids* **153 & 154** (1993) 620.
[32] Dénoyer F., Launois P., Motsch T. and Lambert M., *J. Non-Cryst. Solids* **153 & 154** (1993) 595.
[33] Bancel P., *Philos. Mag Lett.* **67** (1993) 43.